7th Annual Theory and Simulation of Disruptions Workshop,
August 5 – 7, Princeton, NJ

Simulation studies of the ablation of Neon pellets and SPI fragments for plasma disruption mitigation in tokamaks

Roman Samulyak, Nicholas Bosviel, James Yuan, Nizar Nailtho
Stony Brook University
Paul Parks, *General Atomics*

In collaboration with ***Charlson Kim, Brendan Lyons, Lang Lao*** *(GA),* ***Nathaniel Ferraro*** *(PPPL)*

Work supported by SciDAC ***Center for Tokamak Transient Simulations***

Multiple scales of Pellet / Shuttered Pellet Ablation

- Ablation of pellets and SPI fragments in tokamaks is intrinsically a multiscale problem with spatial scales ranging from millimiters (dense clouds near cryogenic pellets) to 10x meters (expansion of ablated material along magnetic field lines), as well as multiple time scales
- A two-level approach is adopted

Local Model

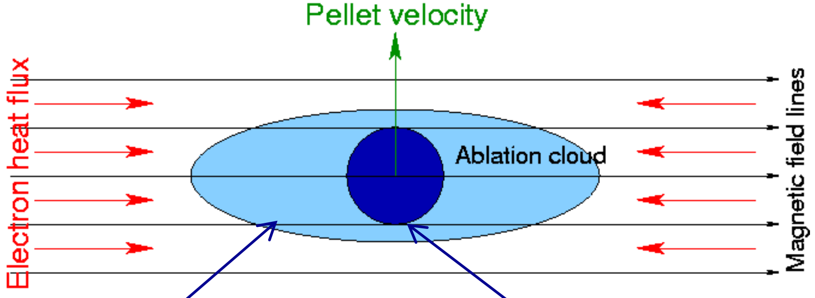

- Phase transition (ablation model) for pellet surface

- Kinetic model for the electron heating of ablated gas
- Low magnetic Re MHD equations
- EOS with atomic processes
- Radiation and Conductivity models
- Pellet cloud charging models
- grad B drift models for ablated material

Global Model

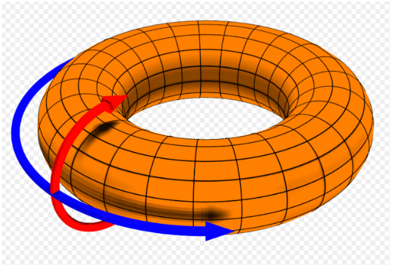

- Extended-MHD
  – Fluid equations for density, momentum, and temperature
  – Faraday-Ampere-Ohm's Law
- Impurity dynamics
  – Continuity eqs. for each charge state
  – Coupled by ionization/recombination
  – Calculates radiated power

Codes that implement Local Pellet Physics Models

FronTier (FT)

- Hybrid Lagrangian-Eulerian code with explicit interface tracking
- Both pellet surface and ablation cloud – plasma interface are explicitly tracked
- 2D axisymmetric simulation of the ablation of single neon or deuterium pellets, computing ablation rates

Lagrangian Particle code **(LP)**

- Highly adaptive 3D code
- Lagrangian treatment of ablation material eliminated numerous numerical difficulties associated with ambient plasma, fast time scales etc.
- Simulate SPI fragments in 3D
- Used for coupling with NIMROD and M3D-C1

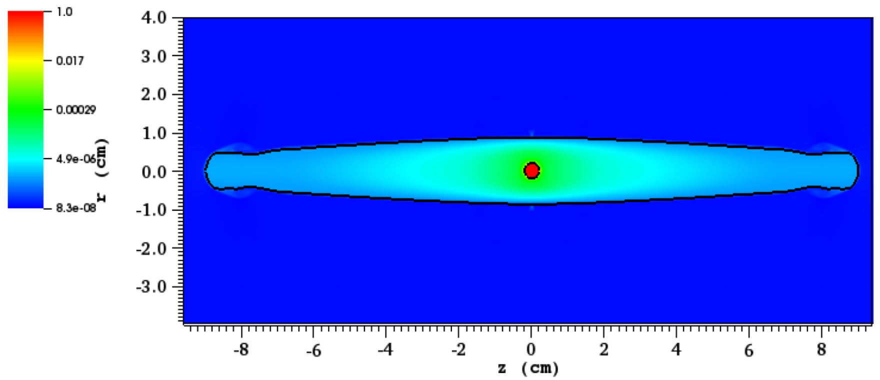

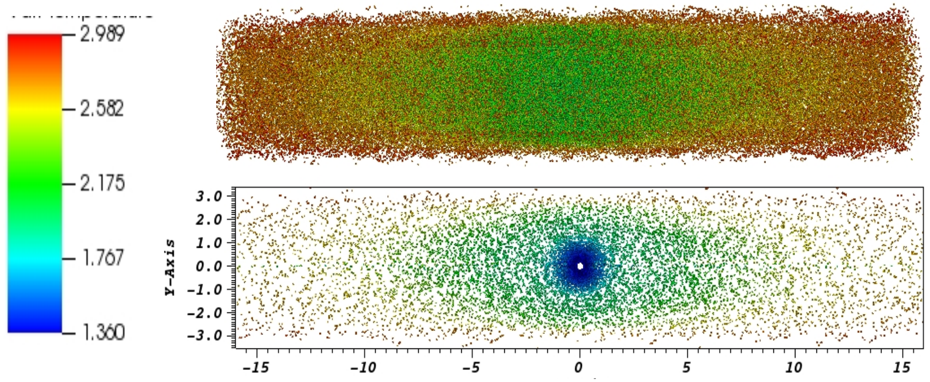

- **Code agreement with certain classes of problems is important for our V&V program**
- The ablation rate = [electron energy flux on the pellet surface / vaporization heat] is effectively **0/0** compared to the order of magnitude of other processes. Small numerical errors in the pellet cloud may significantly change the ablation rate. The ablation rate is also sensitive to other aspects of numerical models (boundary conditions etc.)

Pellet / SPI model based on Lagrangian particles

- A pellet / SPI model has been developed based on Lagrangian Particle (LP) method and software
- Lagrangian treatment of ablated material – eliminated numerical difficulties caused by hot background plasma (see schematic below)
- Ablated material can be tracked during long time / distances
- Optimal and continuously adapting resolution results in small computing time
- LP is usable for hundreds of fragments in 3D
- Significantly reduced stability conditions for Lagrangian flows
- Lagrangian approach provides a natural platform for coupling with global MHD code

- Ref: R. Samulyak, X. Wang, H.-S. Chen, Lagrangian Particle Method for Compressible Fluid Dynamics, J. Comput. Phys., 362 (2018), 1-19.
- Complementary Adaptive Particle-in-Cloud method: X. Wang, R. Samulyak, J. Jiao, K. Yu, Adaptive Particle-in-Cloud method for optimal solutions to Vlasov-Poisson equation, J. Comput. Phys., 316 (2016), 682 - 699.

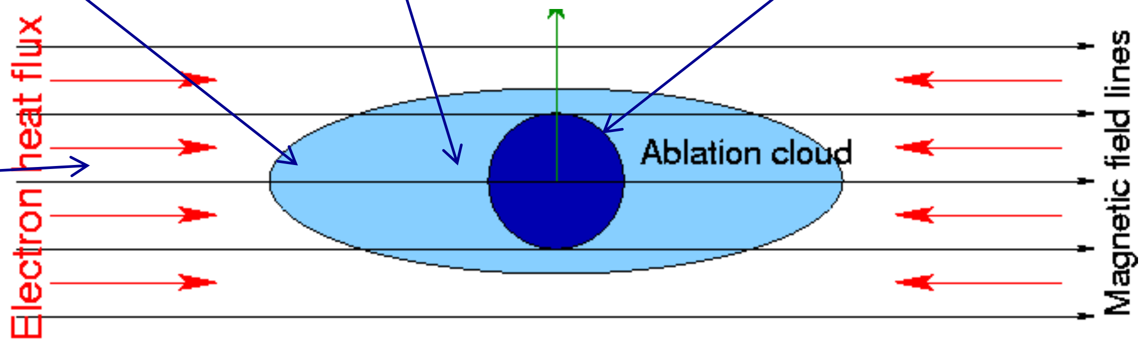

MHD equations in Low Magnetic Reynolds Number Approximation

The ablation cloud expansion is governed by the inviscid, compressible Euler's equations with electromagnetic terms:

$$\frac{\partial \rho}{\partial t} = -\nabla \cdot (\rho \boldsymbol{u}),$$

$$\rho \left(\frac{\partial}{\partial t} + \boldsymbol{u} \cdot \nabla \right) \boldsymbol{u} = -\nabla P + \boldsymbol{J} \times \boldsymbol{B},$$

$$\rho \left(\frac{\partial}{\partial t} + \boldsymbol{u} \cdot \nabla \right) e = -P \nabla \cdot \boldsymbol{u} + \frac{1}{\sigma} \boldsymbol{J}^2 - \nabla \cdot \boldsymbol{q},$$

$$P = P(\rho, e).$$

$\boldsymbol{J} = \sigma(-\nabla\varphi + \boldsymbol{u}\times\boldsymbol{B})$

$\nabla\, \sigma\, \nabla\varphi = \nabla \cdot (\boldsymbol{u}\times\boldsymbol{B}),$

subject to boundary conditions

We assume that the potential is constant in the pellet ablation cloud, and

$$J_\theta = \sigma_\perp u_r B$$

Electron Heat Flux

Parks heat flux model (2019):

$$-\nabla . q = \frac{q_{\infty} n_e(r,z)}{\tau_{eff}} [g(u_+) + g(u_-)]$$

where,

$$g(u) = u^{1/2} K_1(u^{1/2})/4,$$

$$u_{\pm} = \frac{\tau_{\pm}}{\tau_{eff}},$$

$$\tau(r,z) = \int_{\infty}^{z} n_e(r,z')\, dz',$$

$$\tau_{eff} = \tau_{\infty} \frac{1}{0.625+0.55\sqrt{1+Z_*}},$$

$$\tau_{\infty} = \frac{T_{e\infty}^2}{8\pi e^4 ln\lambda}$$

Transverse Conductivity

Transverse electric conductivity (Parks, 2017):

$$\sigma_{\perp} = \frac{9700T^{3/2}}{Zln\lambda + 0.00443T^{2.245}\frac{n^0}{n_e}}$$

In the absence of neutrals,

$$\sigma_{\perp} \rightarrow \sigma_{\perp}^{s} = \frac{9700T^{3/2}}{Zln\lambda}$$

From the tabulated EOS derived from solving the Saha system, the fraction $\frac{n^0}{n_e}$ is readily available in the code via quick look ups.

Equation of State: Saha LTE model. Radiation

The system is closed using either the ideal gas EOS (for benchmarking and verification) or a tabulated EOS generated from solving the Saha equations :

$$\frac{f_{m+1} f_e}{f_m} = \frac{2m}{\rho} \frac{u_{m+1}}{u_m} \left(\frac{2\pi m_e kT}{h^2} \right)^{3/2} \exp\left(-\frac{I_{m+1}}{kT} \right), \quad m = 1, \ldots, Z,$$

along with conservation conditions: $\sum_m f_m = 1$, $\sum_m m f_m = f_e$

Finally,

$$\begin{aligned} P &= (1 + f_e) \frac{\rho kT}{m_a} \\ e &= \frac{3}{2} (1 + f_e) \frac{kT}{m_a} + \frac{1}{m_a} \sum Q_m f_m + \frac{1}{m_a} \sum W_m f_m \end{aligned}$$

- Fully coupled system of nonlinear equations; difficult to solve in each point at each time step of a hydro code
- Both FronTier and Lagrangian Particle codes use tabulated data sets pre-computed by Saha equation solver
- **Non-LTE radiation in thin optical limit** using data sets pre-computed by CRETIN code

Boundary Conditions at the Pellet Surface

- Heat conduction in the pellet can be neglected: the diffusion of heat is slower compared to the removal of pellet material by ablation
  - The surface temperature remains constant (set as 20K)

- Heat flux at the surface:

$$q_{\pm} = \frac{1}{2}\, u_{\pm} K_2\left(u_{\pm}^{1/2}\right)$$

- This heat flux is completely used for phase transition, defining the mass flux:

$$\frac{q_{\pm}}{\varepsilon_s} = \rho v_n$$

- The backward characteristic from the cloud to the pellet surface:

$$\frac{dv_n}{d\lambda_-} - \frac{1}{\rho c}\frac{dP}{d\lambda_-} = \Gamma\frac{\partial q}{\partial z}\text{ , where } \frac{d}{d\lambda_{\pm}} = \frac{\partial}{\partial t} + (v_n \pm c)\frac{\partial}{\partial n}$$

- These equations give a closed system. We solve it to find thermodynamic states and velocity at the pellet surface

Boundary Conditions at cloud-plasma interface

- Physically, the interface between the cloud and plasma form a contact discontinuity across which the pressure is continuous but the density and temperature are not.
- For canonical plasma parameters ($T_e = 2$ kev, $n_e = 7\times10^{13}$), the plasma background pressure is estimated as $P_\infty = 0.64$ bars. This should also be the cloud edge pressure.

- In FronTier, the interface between the ablated material and the background plasma is propagated by solving the Riemann problem in the normal direction to the interface.

- In the Lagrangian particle code, ghost particles are assigned properties of the background plasma and used in incomplete neighborhoods of particles representing the ablatied material at the cloud edge

Grad-B Drift Model for Lagrangian Particle Code

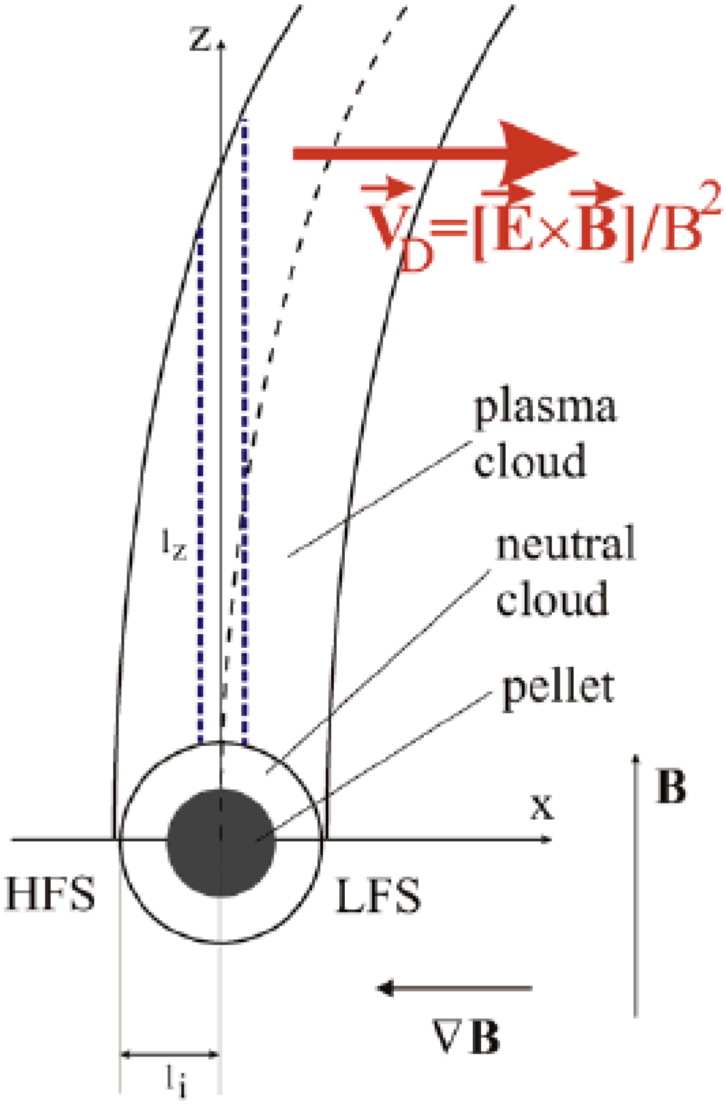

- In close proximity to the pellet, steady state flow with grad-B induced drift can be assumed
- Since the drift is independent of the z coordinate (the electrostatic potential is always assumed uniform along the magnetic field) the equation for the horizontal ExB drift velocity in the x (large-R) direction is governed by the formula [Parks 2000, Rozhansky 1995, 2004]

$$v_D \frac{dv_D}{dx} = \mathrm{J(x)} = \frac{2\langle P - P_\infty \rangle}{R\langle \rho \rangle}$$

where $\langle A \rangle \equiv \int_0^\infty A dz$.

Selected LP Algorithms for SPI

How to compute line integrals for highly non-uniform and dynamic particle systems in the most accurate and efficient way?

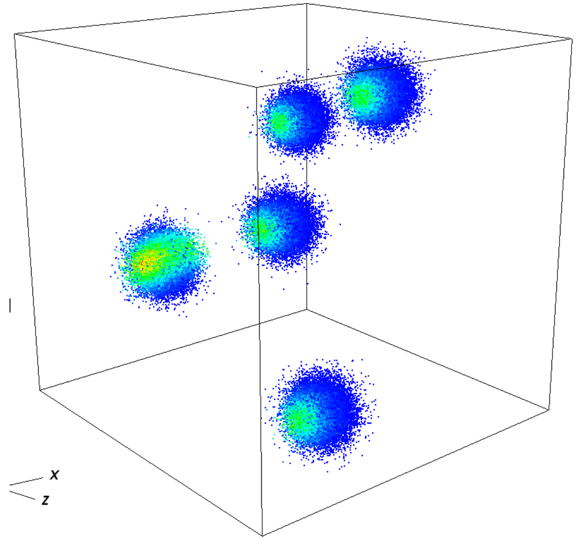

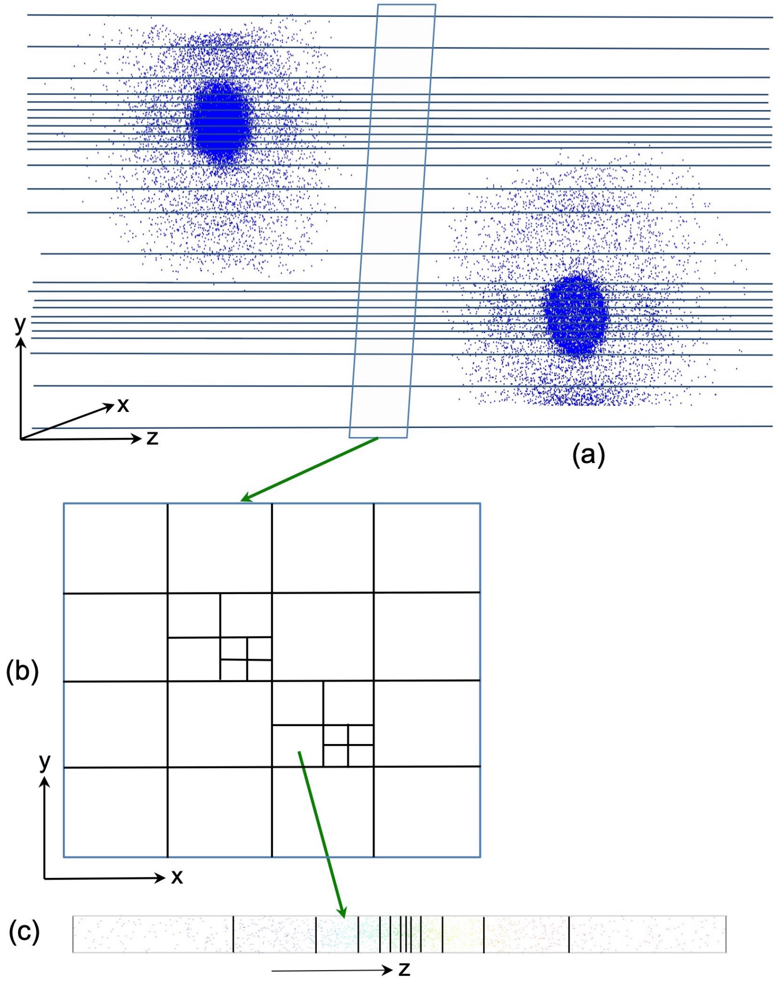

a) 3D distribution of Lagrangian particles in SPI simulation. Horizontal lines schematically depict plasma density integral paths, adaptively refined near pellet fragments.

b) Quadtree data structure, built using Lagrangian particles projected to a transverse plane. Each quadtree cell contains one path for the plasma density integral.

c) Re-distribution of Lagrangian particles in each quadtree cell to 3D using their saved longitudinal coordinate and line integration of density based on a binary tree in the longitudinal direction.

Brief Summary of Results obtained with FronTier and Lagrangian Particle Codes

- Verification: comparison of 1D spherically symmetric FronTier simulations and full 3D LP with spherically symmetric initial conditions with theory

- 2D axisymmetric FronTier simulations and 3D LP simulations in magnetic field
  - No grad B drift model
  - To prevent cutting-off the electron heat flux from the pellet by ablation cloud expanding along magnetic field lines, a finite shielding length is imposed based on theoretical estimates

- 3D LP simulations of pellets and SPI in magnetic field with grad B drift

- Coupling of Lagrangian particle pellet / SPI code with NIMROD and M3D-C1

FT simulations of neon pellet ablation (spherical symmetry)

No atomic processes (ideal gas, 2013 heat flux model):

$n_{e\infty} = 10^{14}$ /cc	$T_{e\infty}$ = 2 keV	$T_{e\infty}$ = 5 keV
r_p = 2 mm	52.33 g/s	248 g/s
r_p = 5 mm	181 g/s	834 g/s

With atomic processes (2013 heat flux model):

$n_{e\infty} = 10^{14}$ /cc	$T_{e\infty}$ = 2 keV	$T_{e\infty}$ = 5 keV
r_p = 2 mm	53.5 g/s (+2.2%)	254 g/s (+2.4%)
r_p = 5 mm	178 g/s (-1.6%)	851 g/s (+2%)

FT simulations of neon pellet ablation (spherical symmetry, cont.)

No atomic processes (ideal gas, 2013 heat flux model):

$n_{e\infty} = 4\text{x}10^{14}$ /cc	$T_{e\infty} = 2$ keV	$T_{e\infty} = 5$ keV
r_p = 2 mm	127 g/s	582 g/s
r_p = 5 mm	439 g/s	2033 g/s

With atomic processes (2013, heat flux model):

$n_{e\infty} = 4\text{x}10^{14}$ /cc	$T_{e\infty} = 2$ keV	$T_{e\infty} = 5$ keV
r_p = 2 mm	110 g/s (-13.4%)	356 g/s (-38.8%)
r_p = 5 mm	334 g/s (-24%)	1629 g/s (-20%)

Neon pellet ablation (spherical symmetry)

Theoretical predictions (2019 heat flux model):

G (g/s)	r^* (cm)	P^* (b)	T^* (eV)
64.44	0.595	6.1038	6.1923

FronTier (2019 heat flux model):

G (g/s)	r^* (cm)	P^* (b)	T^* (eV)
63.77	0.593 cm	6.096	6.212

Lagrangian Particles: G = 64.0 g/s

Ablation rates in the 2D axisymmetric model with MHD forces (2013 heat flux model, FT):

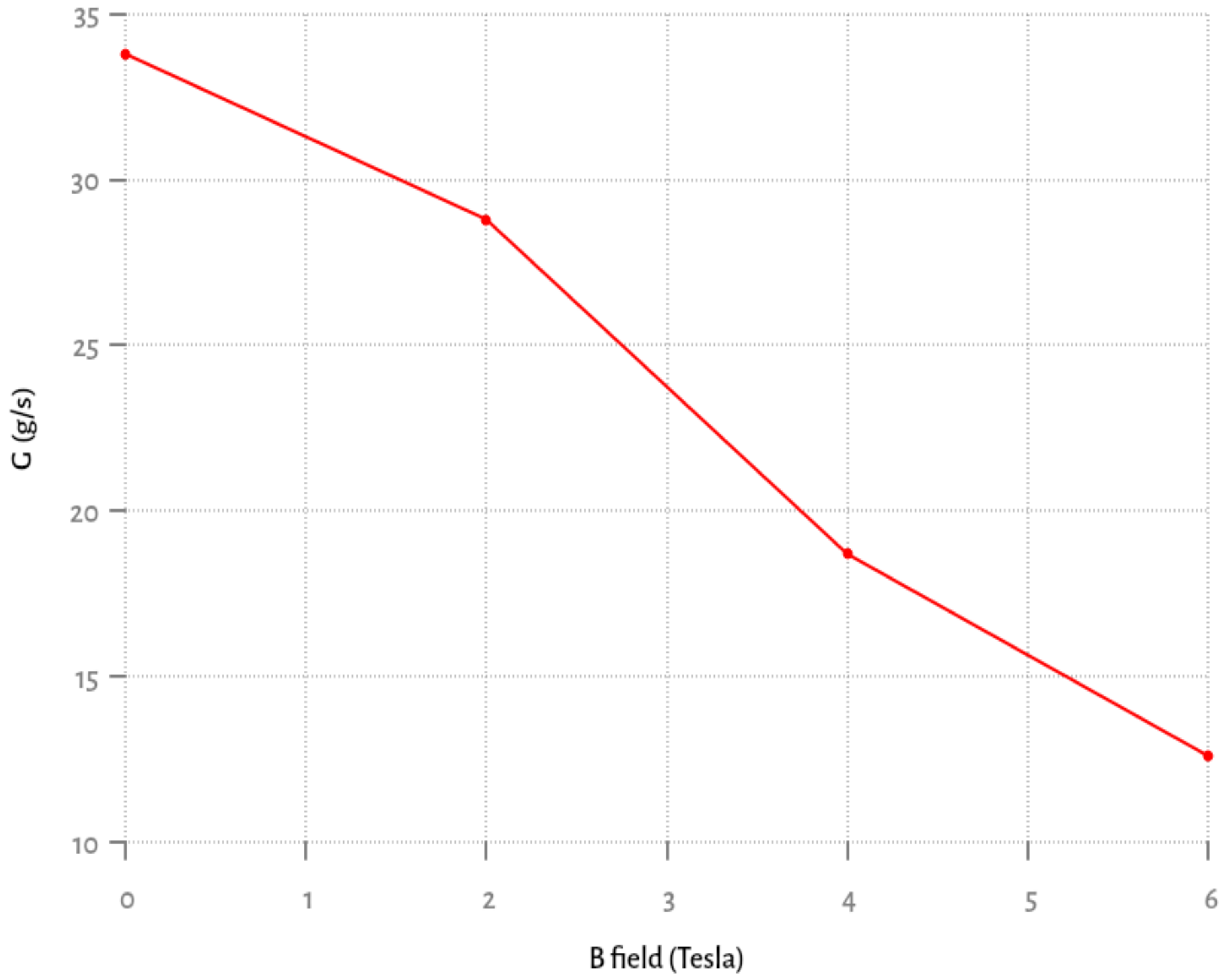

Contrary to the hydrodynamic model where a thin layer of dense material around the pellet provides most of the shielding, MHD effects redistribute the density along the channel leading to stronger shielding and reducing the available energy for pellet ablation.

Compared to the 0T case (no MHD forces), this corresponds to reduction by a factor :

- 1.17 for 2T,
- 1.8 for 4T ,
- 2.68 for 6T.

FT simulations of neon pellet ablation (2D axial symmetry)

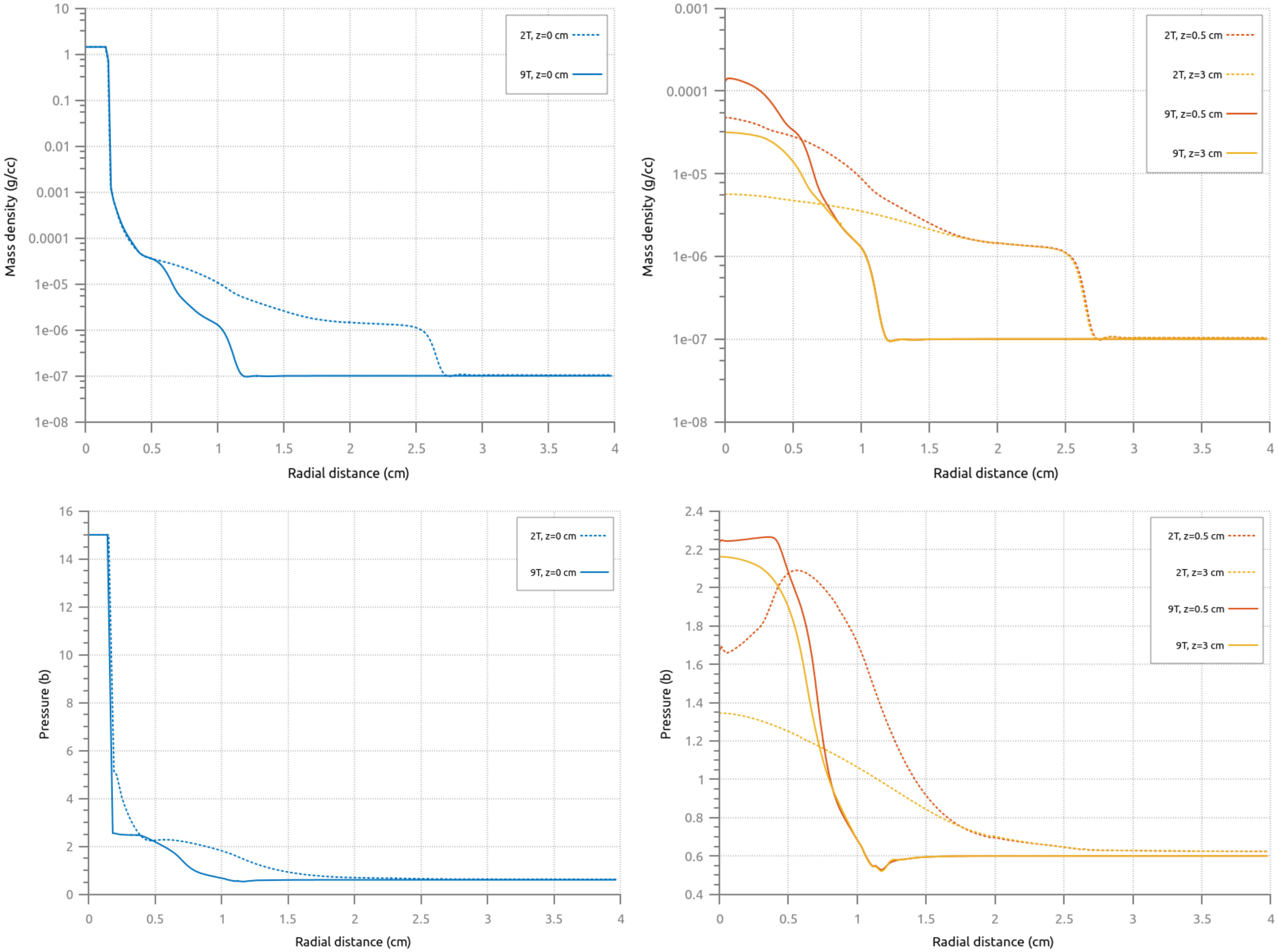

Profiles of density (top) and pressure (bottom) distribution in the transverse direction at different z values for 2T and 9T

FT simulations of neon pellet ablation (2D axial symmetry)

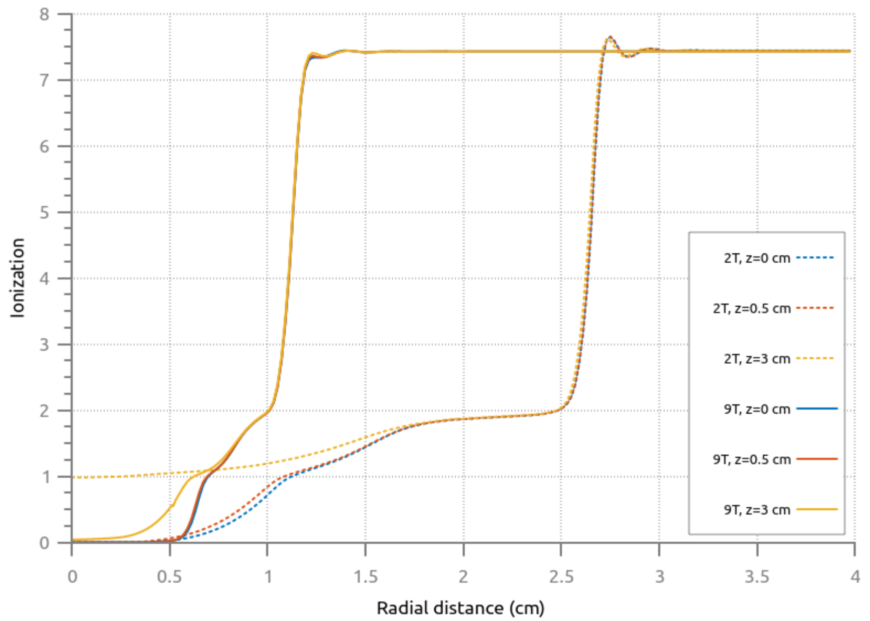

The temperature increase at the cloud edge leads to the higher ionization levels ~ 4.

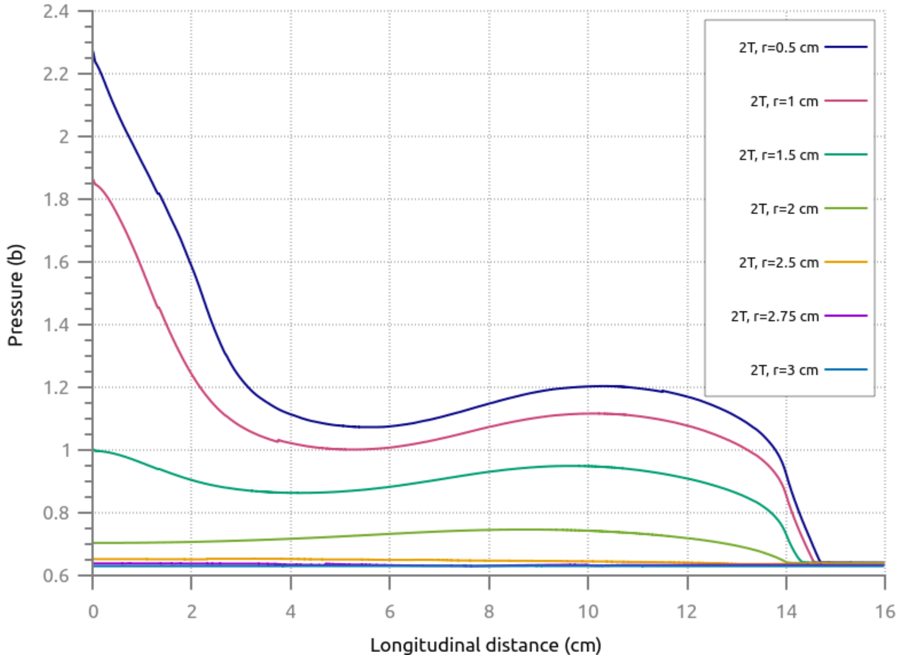

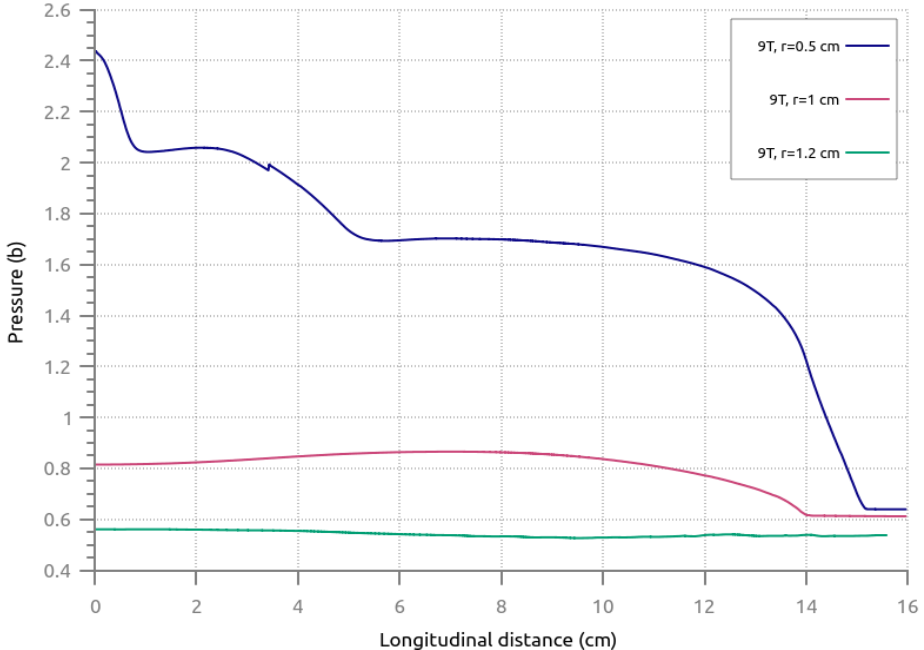

Longitudinal pressure distribution profiles at different r values for 2T and 9T

FronTier 2D simulation: importance of tracking of ablation cloud – background plasma interface

Velocity vector field in 2T field

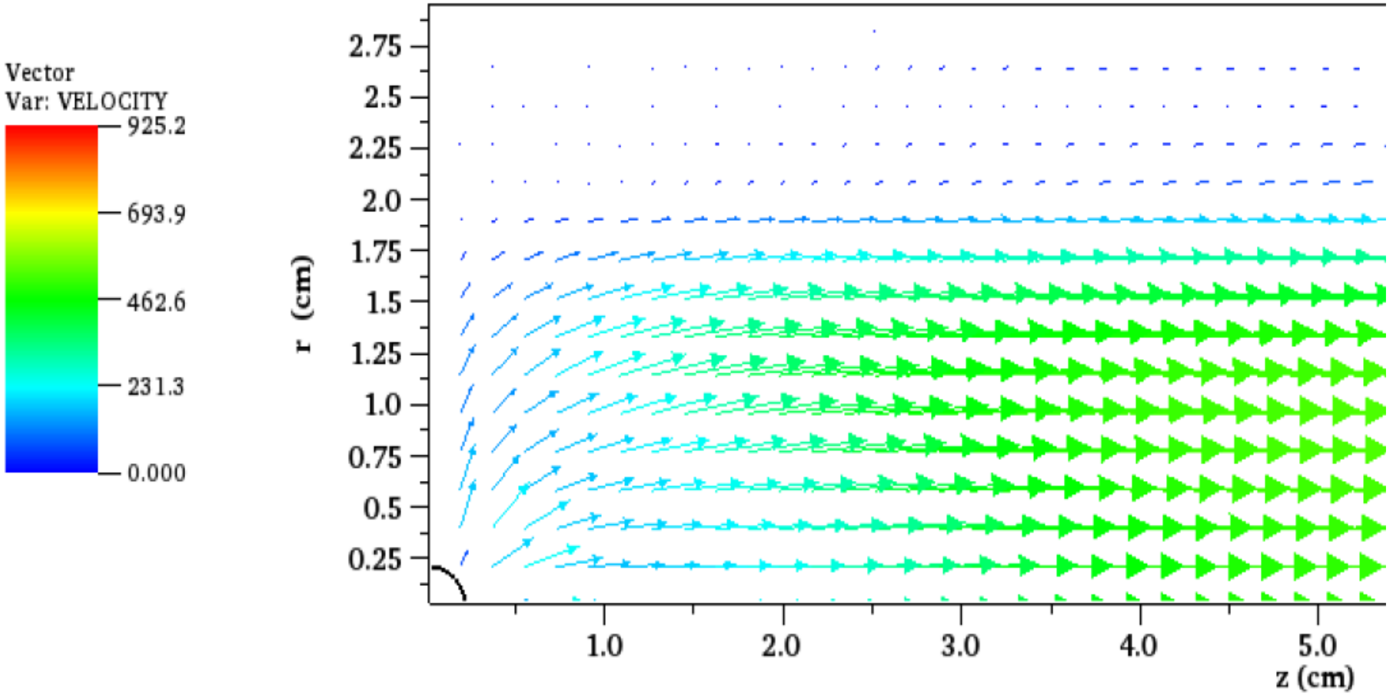

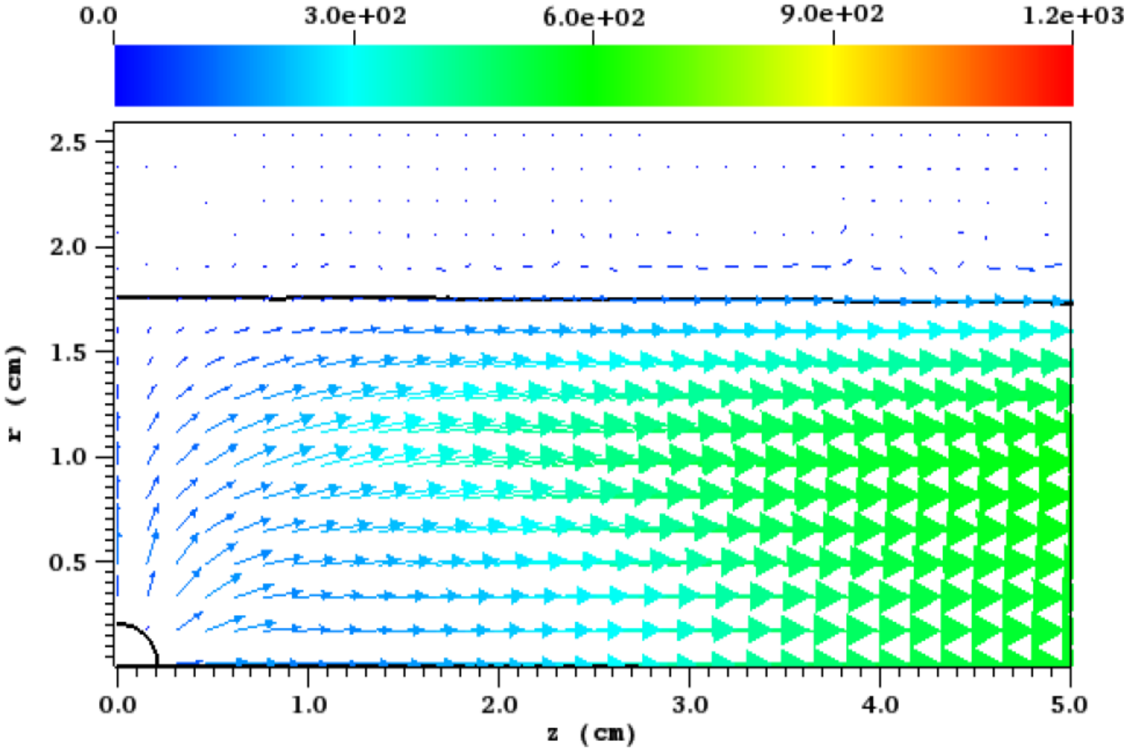

LP simulations of neon pellets by prescribing finite length of the ablation clouds (for comparison with FT), cont.

Distribution of temperature (eV) in (a) 3D cloud, (b) 2D slice through the pellet center, (c) near-surface layer of particles

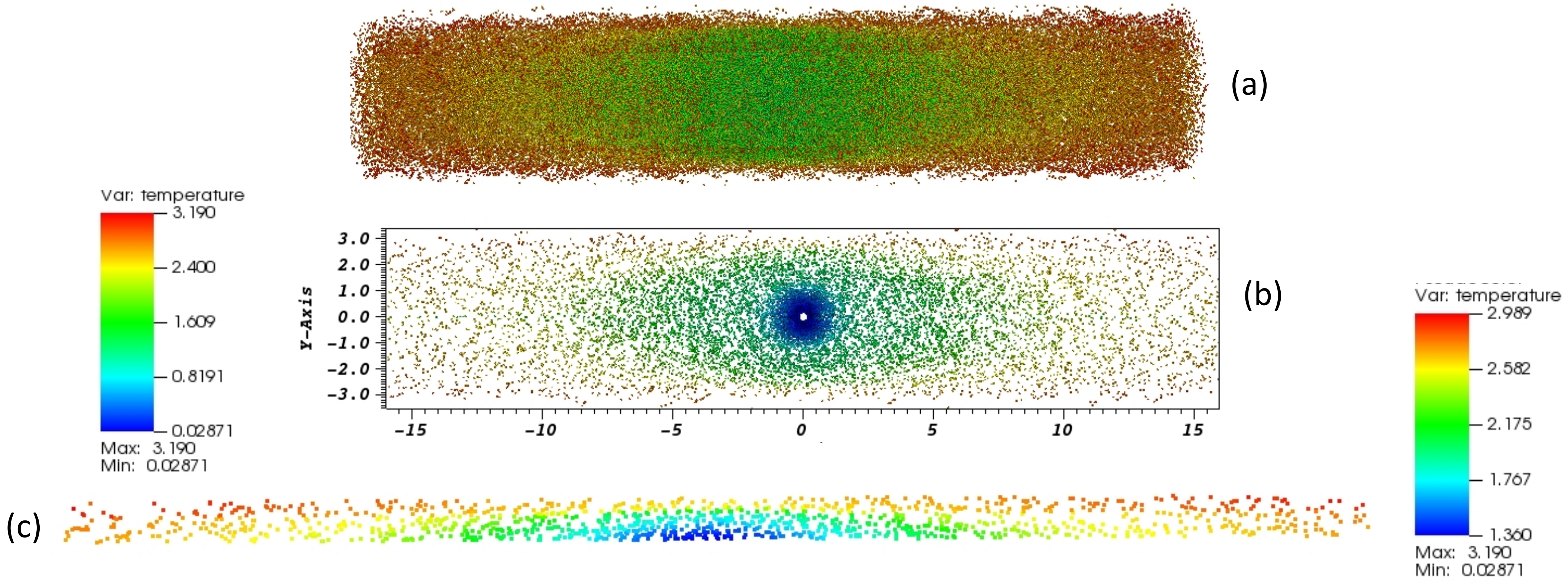

Spherically symmetric: G = 64 g/s

0T: G = 50 g/s, 2T: G = 32 g/s, 6T: G = 27 g/s

Simulation of Neon Pellets with *grad B* drift

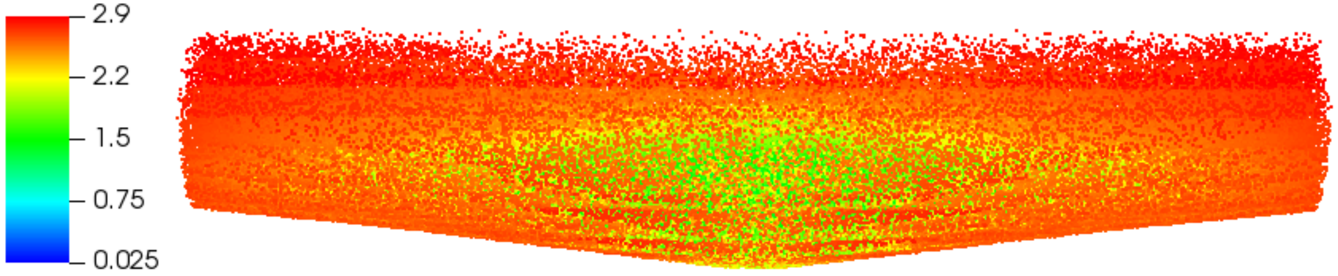

Temperature distribution in the pellet cloud in 2T magnetic field in the presence of grad B drift.
(a) 3D plot
(b) Longitudinal cross-section
(c) Transverse cross-section

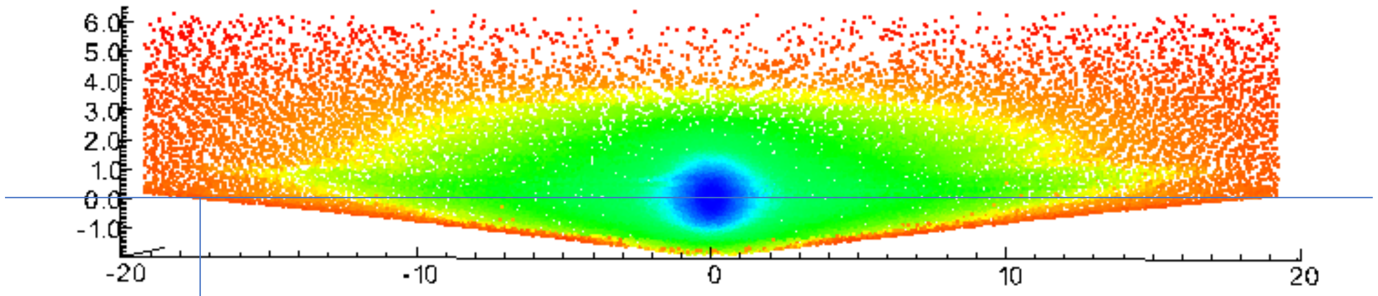

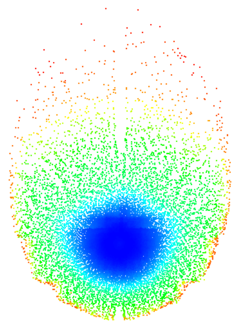

Shielding length due to grad B drift is ~17.3 cm

- Simulations that resolve grad B drift compute the pellet shielding length self-consistently
- For 2mm neon pellet in 2T magnetic field of DIII-D geometry, the computed shielding length is 17.3 cm
- Good agreement with previous theoretical estimates. In previous simulations with prescribed cloud length, the length was chosen in the range 16 – 18 cm
- Ablation rate is only slightly affected in simulations with grad B drift: the ablation rate increased by ~ 4% compared to the fixed length case

Simulation of SPI: estimates of sizes

- Experimental image of the barrel with neon pellet fragments (Baylor, 2018) are shown
- Grad B drift is critical for interaction of SPI fragments

- For DIII-D, the total neon inventory is N_0 = 0.0213 moles
- This amount is contained in in a large pellet with r_{big} = *0.41 cm* (*W* = 20.183 amu is the atomic mass of neon and ρ = 1.444 g/cc is the mass density of frozen neon)
- The pellet is expected to shatter into *N* = 250 smaller fragments. Therefore, the radius of a spherical fragment is $r_{fragment}$ = 0.66 mm
- Assuming a uniform distribution of fragments throughout the cluster stream whose diameter is chosen as d = 30 cm, length L = 30 cm (with the volume of V = 21206 cc), we obtain the distance between fragments as ~4.4 cm

SPI Simulation: no grad B drift

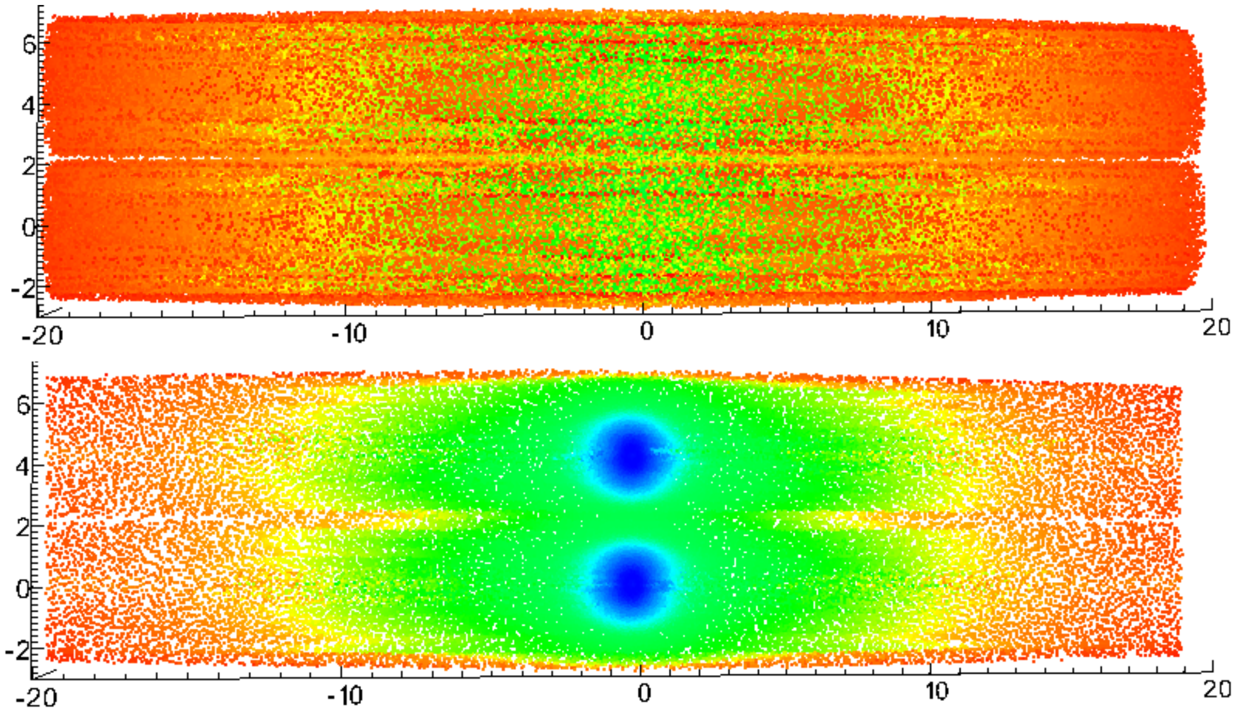

Ablation of large fragments (2 mm)

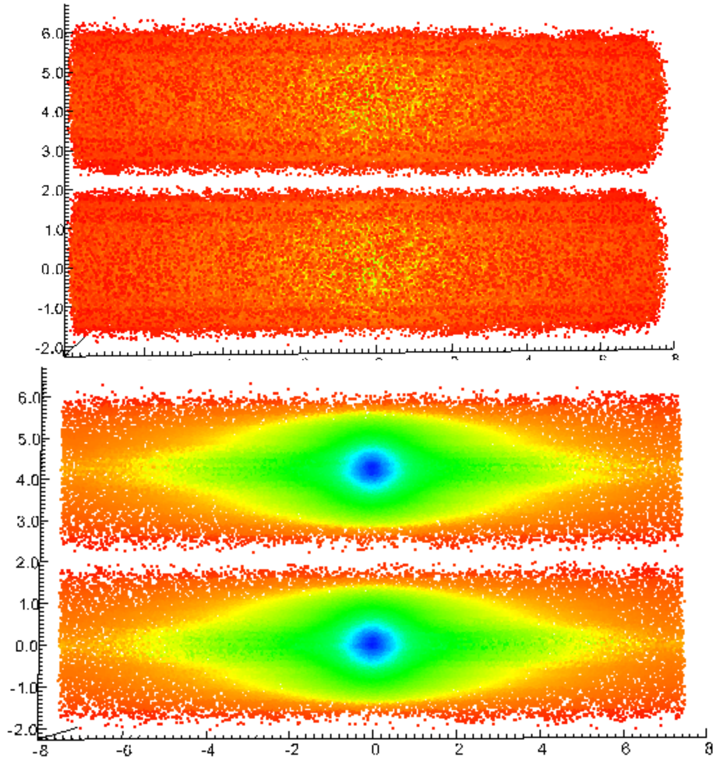

Ablation of small fragments (0.66 mm)

- Simulations without grad B drift show that ablation clouds of pellet fragments separated in the directions transverse to the magnetic field do not interact
  - Even for large fragments (r = 2mm), ablation clouds only touch each other)
  - The ablation rate of each fragment is not affected by the other fragment
  - Small (r = 0.66 mm) fragment create narrow ablation channels separated by ambient plasma

SPI Simulation with grad B drift

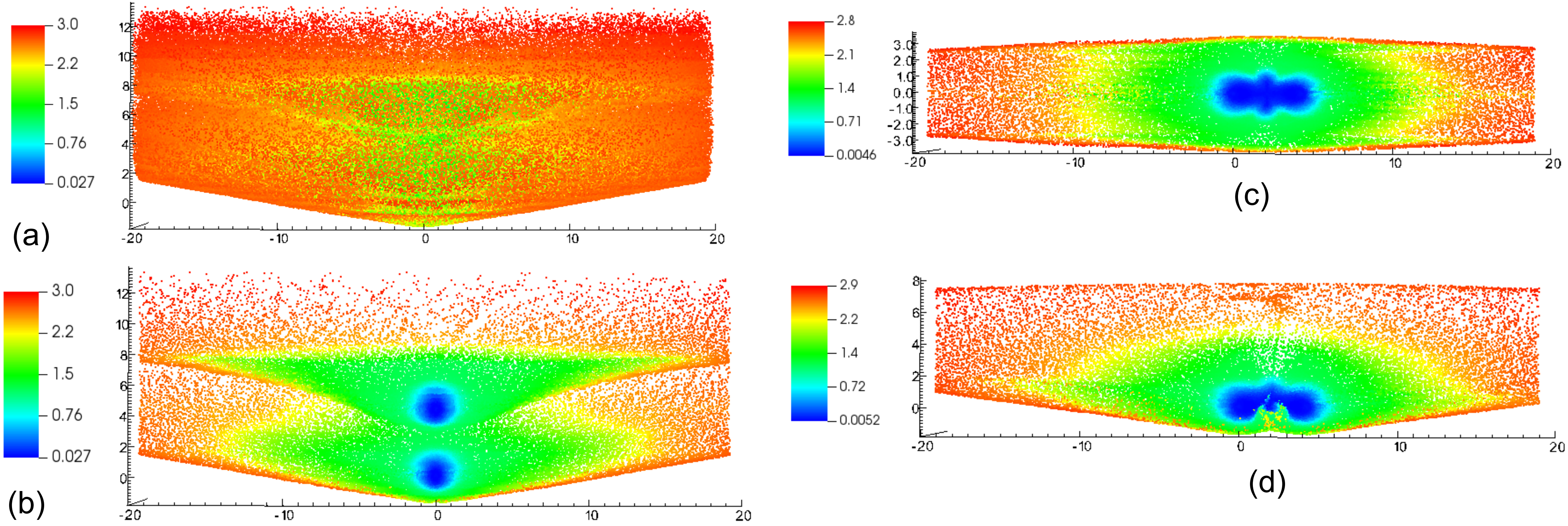

- In the presence of grad B drift, ablation cloud of SPI fragments interact with each other
- The ablation rate of the top fragment is slightly reduced compared to the bottom one. While the effect is small, it may be significant for large number of fragment
- Images on the right show SPI fragments located on the same magnetic field line. (c) No grad B drift. (d) grad B drift included
- For .66 mm fragments,
  - the top fragment ablation rate is reduced by ~ 9 % (a-b)
  - (c) 18% reduction compared to single fragment, (d) 15% reduction compared to single fragment (grad B drift)

Simulation of SPI fragments close to each other

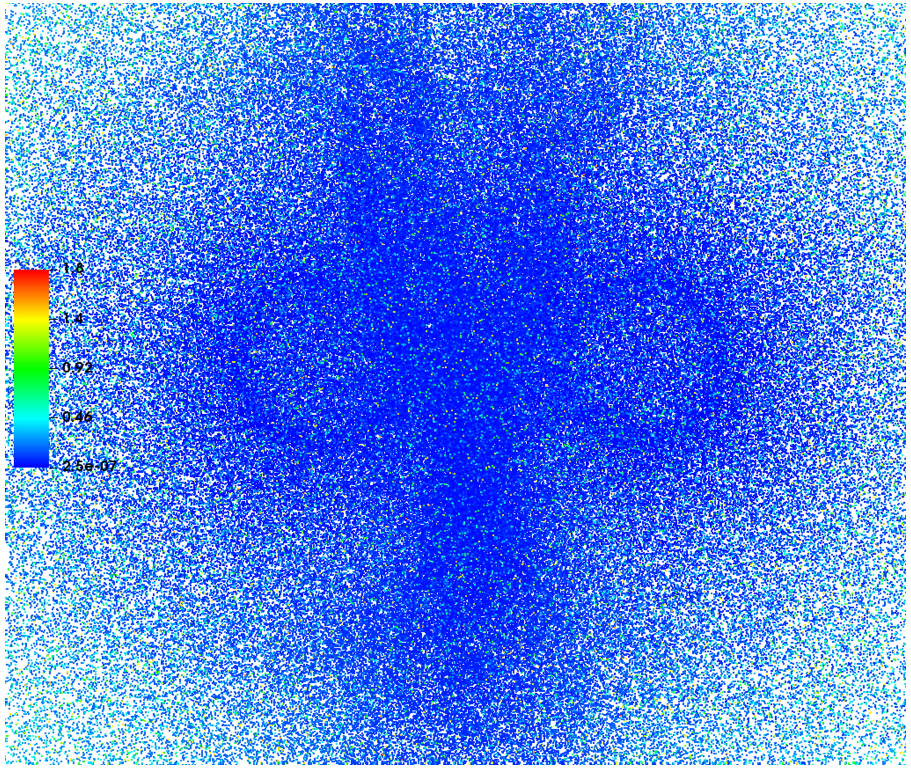

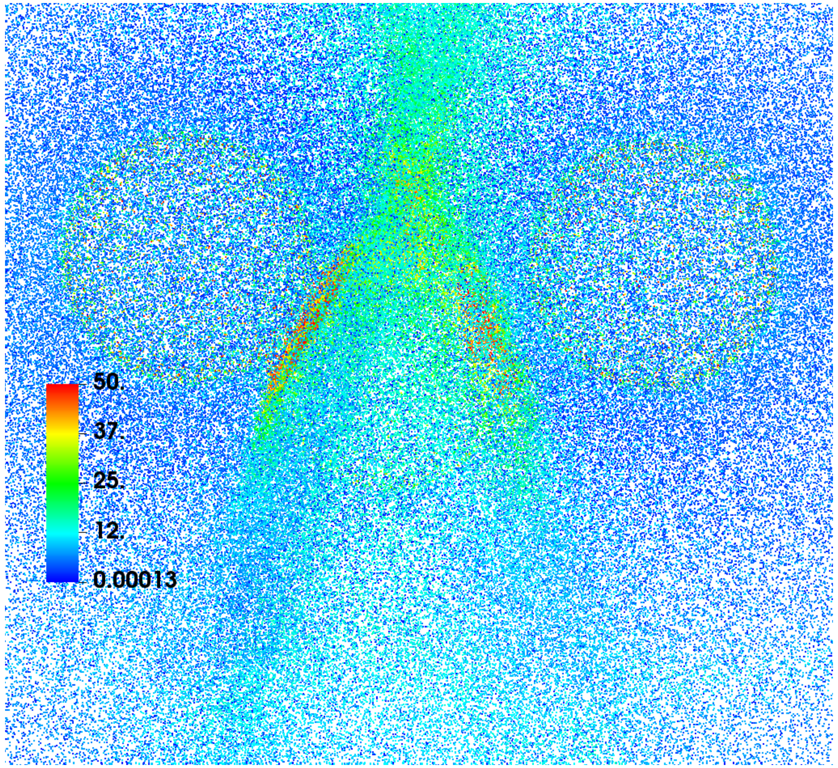

- Simulations of ablation of SPI fragments close to each other shows shock-type waves created by radial ablation flows

Multiscale coupling of Lagrangian particle pellet ablation code with NIMROD / M3D-C1:

- Lagrangian particle approach is beneficial for coupling with global tokamak codes:
    - No need for overlapping domain decomposition typical for grid-based codes
    - Lagrangian treatment of ablated material leads to conservative extraction of ablation flow data.

- Stage 1: Loose coupling. Pre-compute pellet / SPI ablation data and use them as source terms in global MHD codes. The current source terms incorporate information obtained from FT and LP simulations. Work on a detailed pellet ablation database G(B,Ne,T,rp) is undeway.

- Stage 2: Strong coupling

    - Global MHD and LP Pellet / SPI codes will run in parallel on a supercomputer using different nodes / communicators

    - Data exchange will be performed at the time step of the global MHD code (which is >> LP time step)

    - Pellet code data is currently represented by particle states data files; in the future, in terms of basis functions of the global code and the corresponding coefficients will be sent to the global MHD code

    - We have developed a coupling approach that has a well-defined, physics-based separation of scales

Multiscale coupling of Lagrangian Particle Pellet / SPI code to NIMROD and M3D-C1

NIMROD simulation domain showing ablated material obtained from LP code

LP simulation of pellet ablation cloud

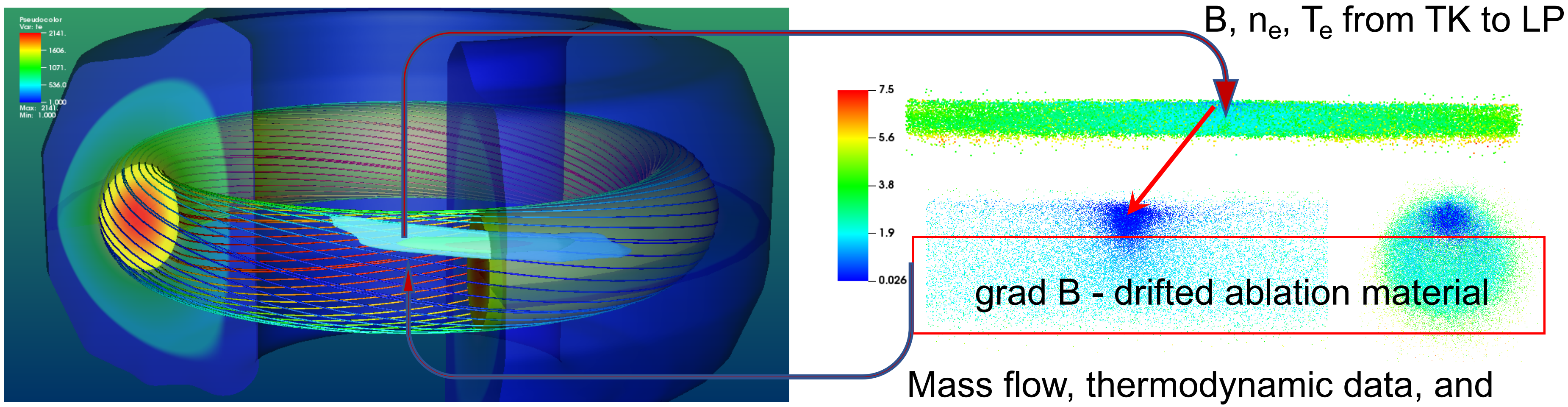

Mass flow, thermodynamic data, and energy sinks from LP to TK

- **Grad B drift provides physics-based separation of scales for coupling**

- LP code evolves self-consistently the entire ablation cloud that provides pellet shielding
- grad B drift model in the LP code propagates ablated material across magnetic field lines, establishing the cloud shielding length. Ablated material that drifted beyond the main ablation cloud is transferred to the tokamak code, together with thermodynamic data and energy sinks. Particle representation ensures conservative mass transfer
- LP code obtains the magnetic field and electron density and temperature from the tokamak code

- LP data input has been successfully incorporated in NIMROD

Simulation Studies of Parallel Flow Problem

Schematic: deuterium plasma column interacting with background plasma electrons

- Simulations of plasma column in magnetic field (no pellet ablation / particle source)
- Simulation purpose: study of the propagation of ablated material along magnetic field lines
- Compare with 1D PRL code simulations
- Study possible mechanisms leading to soliton-like signals in recent experiments

Deuterium column:
ne = ni = 4x10^16 /cc
Te = 2 eV
half-length of cloud = 10.8 cm

Background plasma:
Te_inf = 500 eV
ne = 4x10^13 1/cc, reduced to 6.4x10^12 1/cc by the electrostatic shielding

Simulation Studies of Parallel Flow Problem

- Understanding of long-range propagation of ablated material along magnetic field lines is a high-priority task
- 3D Lagrangian particle simulations of a plasma column expansion up to 10 m in length are in very good agreement with 1D PRL code results in terms of expansion distances and longitudinal profiles of thermodynamic states

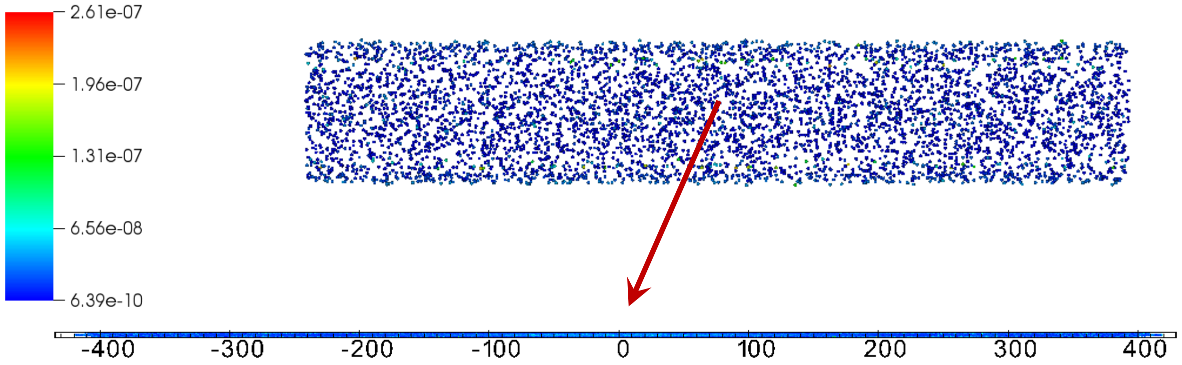

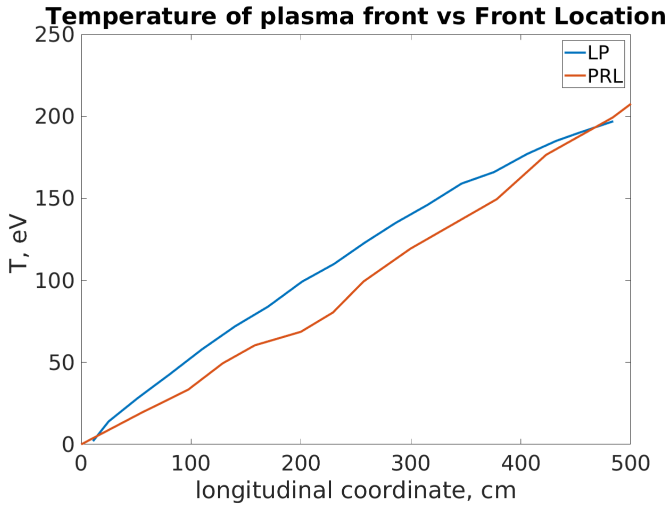

Top: temperature in the front part of plasma column vs the front location using 3D LP with Saha EOS and 1D PRL with ideal gas EOS. Bottom: front of plasma location in time.

Work in progress:

- A set of 1D equations was developed that incorporate changing magnetic field
- These equations are being implemented in 1D version of the Lagrangian Particle code
- 1D simulations will be compared with full 3D Lagrangian particle simulations of parallel flow in changing magnetic field

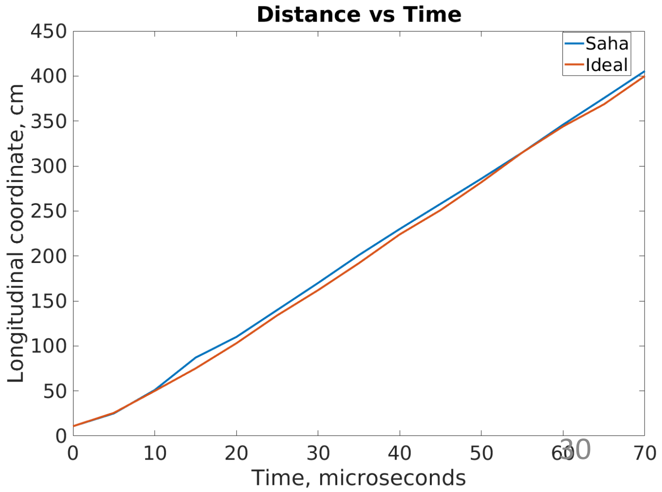

Summary and Future Work

- Detailed physics model for pellet ablation based on front tracking (2D axisymmetric), and 3D pellet / SPI code based on Lagrangian particles have been developed
  - Recent improvements of physics models and numerical algorithms (explicit tracking of ablation cloud in FT, grad B model in LP, improved adaptive K-tree algorithms)
  - Performed verification simulations and code comparison
  - Verification: excellent agreement of theoretical predictions and simulations using both codes for spherically-symmetric case

- Performed FT and LP simulations that quantify the influence of plasma parameters and tokamak magnetic fields on the ablation rate of neon pellets. Parallel ablation flow / long range expansion

- Started 3D simulations of SPI; grad B drift is critical for the interaction of ablation flows of individual fragments

- Developed a multiscale coupling method of with M3D-C1 and NIMROD
  - Well-defined, physics-based separation of scales
  - LP data input has been successfully incorporated in NIMROD

- Future work:
  - Continue V&V; perform runs with fully coupled codes
  - New physics: DT / neon mixtures, kinetic heating by runaway electrons